Int. J. Electrochem. Sci., 14 **(2019)** 777 – 791, doi: 10.20964/2019.01.70

International Journal of
ELECTROCHEMICAL
SCIENCE
www.electrochemsci.org

Preparation and Properties of Core-shell Structure Fluorine-modified Acrylic Anticorrosion Coatings

Xia Wang[*], *Hui Wang, Zhang Dai-xiong, Li Hou, Huan Jiang*

Material science and Engineering School, Southwest Petroleum University, Chengdu 610500, People's Republic of China
[*]E-mail: swpi_wx@126.com

Received: 1 September 2018 / *Accepted:* 10 November 2018 / *Published:* 30 November 2018

A core–shell fluorine modified polyacrylate hybrid latex was successfully prepared by seed emulsion polymerization. The emulsion was characterized by fourier transform infrared spectroscopy and transmission electron microscopy. After the emulsion was prepared on the surface of stainless steel, the surface of the coating was observed. The heat resistance of the coating was analyzed by thermogravimetry, and the corrosion process of the coating was studied by electrochemical experiments. The results showed that the crosslinking degree and the heat resistance of the coating has been improved. The corrosion potential was increased from -0.46 V to -0.17 V and the current density was reduced from 2.50×10^{-6} A/cm^{-2} to 5.54×10^{-8} A/cm^{-2} compared with the unmodified coating. The improvement of its anti-corrosion performance is mainly due to the improvement of the shielding effect and surface hydrophobicity. Due to its special core-shell structure, the addition of fluoromonomer to achieve this effect is only 2.36%.

Keywords: Coating, Fluorine-modified acrylic, Corrosion protection, Stainless steel, Surface property

1. INTRODUCTION

Stainless steel has been widely used in industrial and construction industries because of its favorable corrosion resistance molding properties. However, 304 stainless steel is prone to corrosion in the presence of chloride ions, and the corrosion rate may even exceed that of ordinary carbon steel[1]. That restricts the use of stainless steel. Stainless steel must be kept dry and clean when used outdoors[2]. Commonly used corrosion protection methods in industrial production include adding corrosion inhibitors, cathodic protection and coating protection[3~6]. Applying a coating with a low surface energy on the surface of stainless steel can solve the problem of corrosion of 304 stainless steel. In response to the requirements of environmental protection, anti-corrosion coatings are changing to water-based.

Water-based paints use water as a dispersant and do not produce organic contaminants during film formation[7]. Acrylate emulsions are widely used as film-forming materials for coatings due to their excellent performance at low cost[8]. However, compared with conventional solvent-based coatings, acrylic coating also have problems such as poor water resistance, poor heat resistance and high surface energy[9].

Recently, fluoropolymers have attracted considerable attention because of their unique properties such as excellent surface hydrophobicity, good chemical, thermal and photochemical stability[10~15]. Fluoroacrylate copolymers have excellent film forming capabilities and have been used in biomaterials, microelectronics, anti-fog and anti-corrosion applications. However, the relatively high market price of fluorine-containing monomers has limited their practical application. How to maintain excellent physical qualities becomes a very tricky issue for the chemical properties of fluorinated polymers by using small amounts of fluorinated monomers. The solution to this problem is to synthesize core-shell fluorinated polyacrylates. In this case, the fluorinated polyacrylate is composed of fluorine-free nucleus and fluorinated shell. For this particular structure, the fluorine-containing group is favorably transferred to the surface during the film formation process, giving the polymer film an excellent film. The waterproof and oilproof performance. Zhou[16] modified acrylate emulsion with dodecafluoroheptyl methacrylate (DFMA) and studied the modified latex film. Compared with the unmodified latex film, the modified latex film not only has a lower surface energy, but also has a significant increase in its heat resistance. Ting[17] used a one-step microemulsion polymerization to prepare a fluorine-modified acrylate emulsion and reached the same conclusion.

As far as we know, there have been few reports on the corrosion resistance of fluorinated polyacrylic coatings with core-shell structures. The main purpose of this study is to investigate the application value of fluorinated polyacrylate coating with core-shell structure in corrosion protection. A fluorinated acrylate emulsion was prepared by simple seed emulsion polymerization. During the preparation process, dodecafluoroheptyl methacrylate (DFMA) was used as a fluoromonomer, methyl methacrylate (MMA), butyl acrylate (BA) as a polymerization monomer for acrylic acid. The composition and structure of the polymer emulsion was confirmed by fourier transform infrared spectroscopy and transmission electron microscopy. The properties of the coating were tested and the electrochemical properties were analyzed primary.

2. EXPERIMENTAL

2.1 Materials

Methyl methacrylate (MMA), butyl acrylate (BA), acrylic acid (AA) were purchased from Chengdu Kelong Chemical Factory. Dodecafluoroheptyl methacrylate (DFMA) was obtained from Shang Fluoro Company. Alkylvinylsulfonate (AVS), alkylphenol ethoxylates(OP-10) and ammonium persulfate (APS) was product of Chengdu Kelong Chemical Factory.

2.2 Synthesis and characterization of the fluorinated acrylate

The recipes for the synthesis of the fluoridated acrylate emulsion were summarized in Table 1. Take 0.26g AVS and 0.13g OP-10 was added to 30ml of demonized water mixed and stirred by 50℃ for 10 min. 12.00g of BA, 6.00g of MMA and 1/3 emulsifiers were mixed in a beaker followed by vigorous stirring to form pre-emulsion I. Similarly, 6.00g of BA, 8.00g of MMA, 0.50g of AA, 4g of DFMA and 1/3 emulsifiers were mixed in a beaker and then vigorously homogenized to form pre-emulsion II.

The initiator was prepared by dissolving 0.3g of APS in 10ml of demonized water. A four-necked round-bottomed flask equipped with a constant pressure dropping funnel, a reflux condenser, a thermometer and a mechanical stirrer was filled with the remaining emulsifier, 1/3 initiator and 1/2 pre-emulsion I and stirred at a rate of 250 rpm at 75℃. When the emulsion acquired a uniform blue color, remnant pre-emulsion I were added dropwise into the reacting mixture, which lasted for about 2h. Finally it warmed to 85℃ insulation for 1h. After the insulation was completed, the temperature was lowered to 80℃ and pre-emulsion II were dropped slowly for 3~5h. Increased temperature to 90℃ for 1h. Adjusted pH 7~9 after dropping to room temperature.

Table 1. Formulations for fluorine modified polyacrylate emulsion.

Sample	S0	S1	S2	S3	S4
BA(g)	18	18	18	18	18
MMA(g)	14	14	14	14	14
AA(g)	0.5	0.5	0.5	0.5	0.5
DFMA(g)	0	1	2	4	6
AVS(g)	0.26	0.26	0.26	0.26	0.26
OP-10(g)	0.13	0.13	0.13	0.13	0.13
APS(g)	0.3	0.3	0.3	0.3	0.3
Deionized water(g)	60	60	60	60	60

2.3 Stainless steel 304 treatment

Stainless steel 304 samples were prepared as squares with the dimensions 40mm×13mm×2mm and polished with emery paper of different grades (240, 400, 800, 1200 and 2000). The samples were cleaned with acetone and rinsed with distilled water, dried in the air and stored in desiccators prior to use. The emulsion was coated on the steel plate with a 40 μm bar coater. The film was dried in 60° C environment for 5 hours and the moisture inside the latex film was removed. The dried film was annealed at 120°C for 30 minutes.

2.4 Characterization

The chemical recipes of fluorine modified polyacrylate emulsion was investigated by a Fourier transform infrared (FT-IR) spectrometer from Thermo Scientific. The spectrum was recorded in the

wavenumber range of 500 ~ 4000 cm^{-1} using KBr powder.

Transmission electron microscopy (TEM) of the fluorine modified polyacrylate seed emulsion particles was carried out with a Hitachi HT-7700 electron microscope (Hitachi Limited, Tokyo, Japan) at a voltage of 100 kV.

Scanning electron microscope (SEM) and energy dispersive spectrometer (EDS) for analysis of surface topography and elemental recipes was used ZEISS EV0 MA15 from Carl Zeiss Jena.

The coating was analyzed using a DSC823 TGA/SDTA85/e (METTLER TOLEDO) instrument. DSC temperature range was -25 to 200℃ thermogravimetric under nitrogen atmosphere. TGA was performed using a thermal analyzer under nitrogen atmosphere at a heating rate of 10 °C/min to 700 °C.

Contact angle measurements were performed with a contact angle goniorneter (OCA 25, Dataphysics Instruments GmbH) using the sessile drop method with a microsyringe at room temperature. Static contact angles were obtained from 5μl water droplets on surface of coating.

The coating is subjected to electrochemical impedance spectroscopy (EIS) testing after drying. It was coated with paraffin and a 1cm×1cm working area was emptied for experimentation. An electrochemical workstation was used for the experimental apparatus. The electrolyte solution was a 3.5% NaCl solution. The coated stainless steel was a working electrode, the platinum electrode was an auxiliary electrode, and the saturated calomel electrode was a reference electrode composed of a three-electrode system. The sinusoidal wave with a voltage amplitude of 5mv is applied to the electrochemical impedance measurement process and the frequency was between 10^{-2} and 10^{5}Hz.

3. RESULTS AND DISCUSSION

3.1 Synthesis of Fluorinated Acrylate Emulsion

The FTIR curve for the fluorine modified polyacrylate emulsion was showed in Figure 1. The -C-O absorption peak appeared at 3449 cm^{-1}. The stretching vibration peak of $-CH_2$ and $-CH_3$ groups appeared at 2955 cm^{-1}, and the stretching vibration absorption peak of ester group -C=O appeared

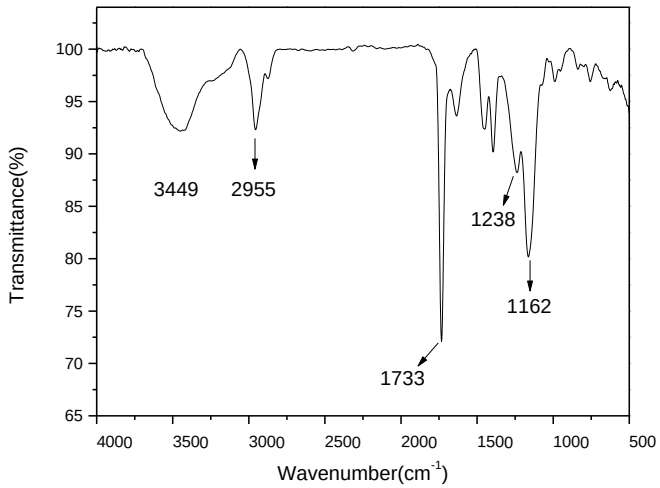

Figure 1. FTIR spectrum of fluorine modified polyacrylate emulsion.

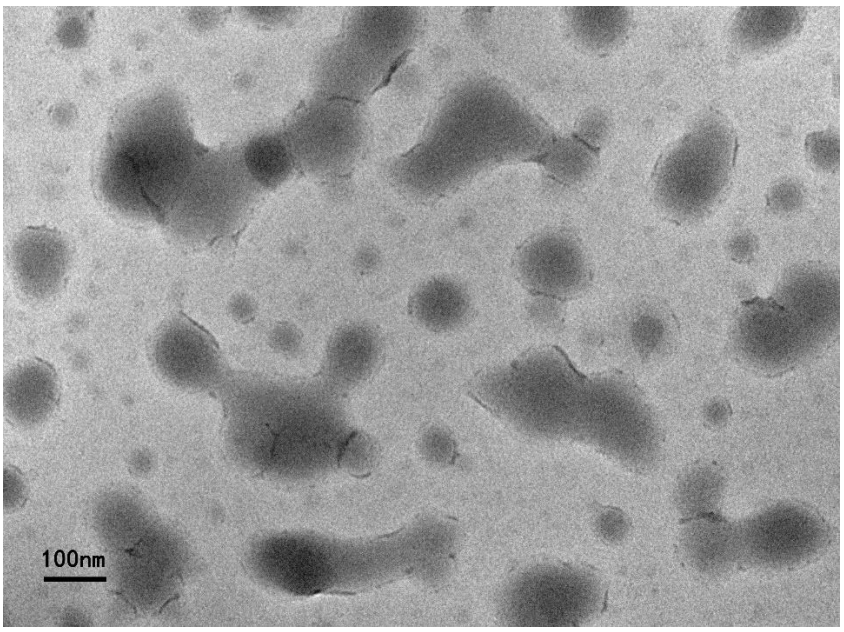

Figure 2. TEM image of latex particles of fluorine modified polyacrylate emulsion.

at 1733 cm^{-1}. $-CF_2$ ($-CF_3$) appeared at 1238 cm^{-1} and 1162 cm^{-1}[18, 19]. The characteristic peaks demonstrated that the fluoromonomer has successfully participated in the polymerization of the emulsion. InF the Figure 1, there was no strong characteristic peak of the C=C, demonstrating that the monomer reaction was completed.

The morphology of the latex particle was shown in Figure 2. It could be seen that the fluorinated polyacrylate particle exhibited a typical core-shell structure, which was evident from the significant contrast between core (light regions) and shell (dark regions) because of their different electron penetrabilities[20, 21]. The size of latex particle was approximately 200 nm, while the shell thickness was approximately 10 nm.

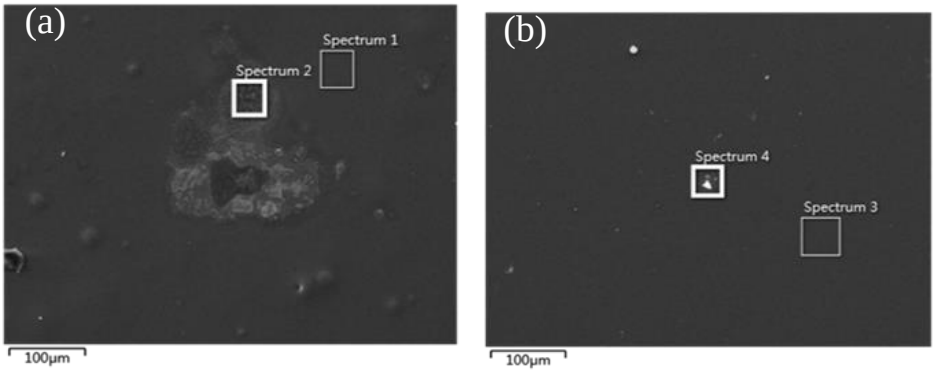

Figure 3. SEM images of polyacrylate coating (a) and fluorine-modified coating (b).

3.2 Surface analysis

Table 2. Atom content of component on surface of polyacrylate coating and fluorine-modified coating.

Element(Atomic %)	C	O	Fe	F
Specturm 1	83.99	15.19	0.82	0
Specturm 2	74.24	16.34	0.99	0
Specturm 3	79.36	14.25	0.54	2.25
Specturm 4	80.20	15.66	1.34	1.89

The EDS test was performed on the coating as showed in Figure 3. It could be seen that fluorine-free acrylate coating had many surface defects, such as pores and large area block defects in Figure 3a. That was resulted from the large amount of emulsifier and the moisture content of the acrylate emulsion during the coating formation[22]. With an evaporation treatment, the polymer particles were densely packed and coalesced into a continuous coating. Since the emulsifier could not evaporate with moisture so the particles accumulation was hindered, which would result of defects in the coating. In figure 3b, there were also some defects in the coating after adding DFMA. Compared with the sample of Figure 3a, the modified coating was significantly denser and smoother, with a large-area of reduced defects and increased density. The elemental analysis of the smooth surface and drawbacks for the coating were given in the table 2. The presence of F on the surface of the fluoropolymer film indicates a successful participation of DFMA in the polymerization. The content of iron in the defects of the fluoridated acrylate emulsion was higher than that in the acrylate emulsion containing no DFMA. It could be concluded that the emulsifier in the fluoridated acrylate emulsion did not accumulate into large amounts but rather was relatively uniformly dispersed on the surface of the film, so the resulting defects were deeper than the large area blemish at the acrylate emulsion defects[23].

3.3 Contact angle analysis

Water contact angle was commonly employed for evaluating the surface hydrophobic properties[24]. The influence of the additional amount of fluorine-containing monomers on the contact angle was analyzed by varying the DFMA content, as showed in the Figure 4. It could be seen that the coating without DFMA added had hydrophilicity and a water contact angle of 36.3°. After the fluorine modification, the hydrophobic property of the coating had been significantly improved and the water contact angle had increased to about 80°. With the increase of DFMA content, the contact angle of water on the coating surface had showed an increasing trend, but the change of the contact angle was getting smaller after the content is increased to 2.36%. Because the fluorine content on the surface of the coating tended to be saturated, the surface fluorine content would not increase with increasing DFMA content.

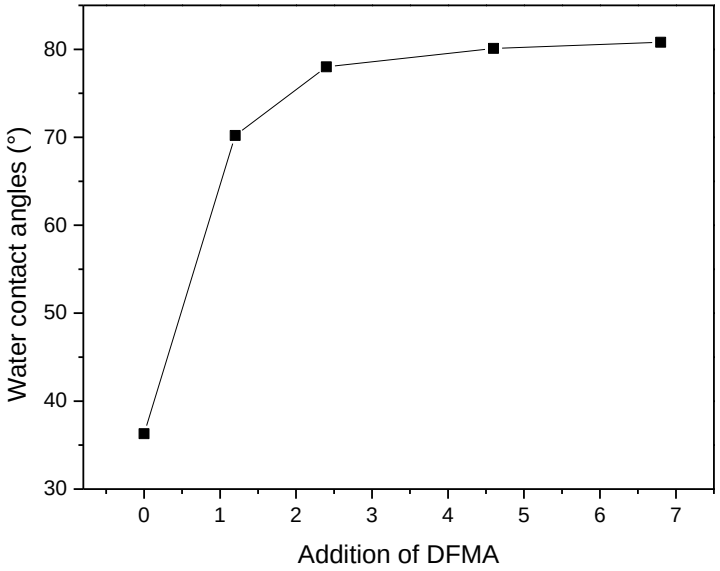

Figure 4. Effect of amount of DFMA on hydrophobic of steel surface coating.

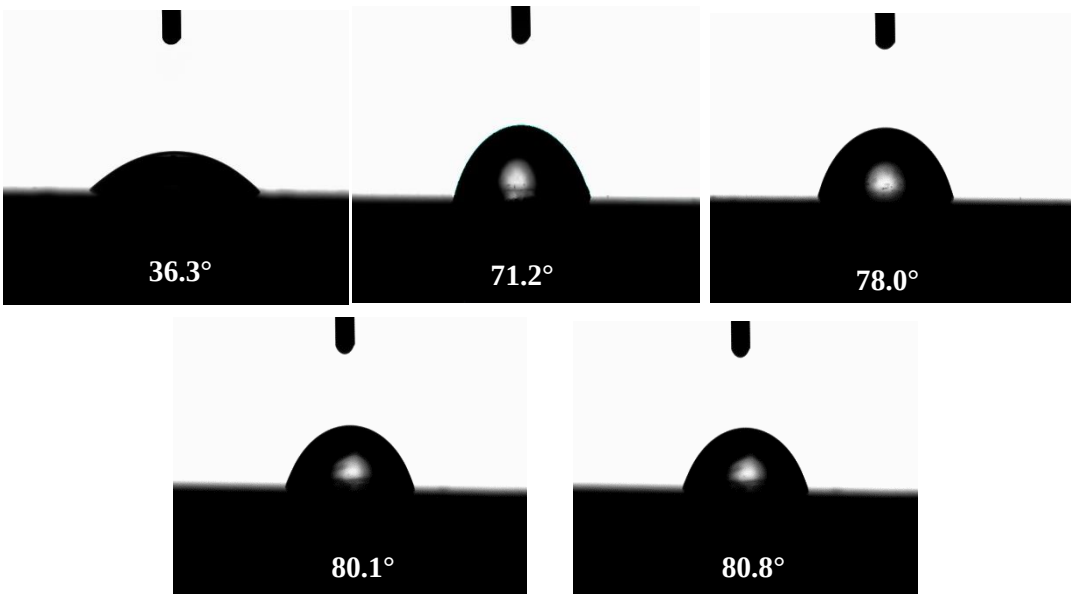

Figure 5. Static water contact angle with different DFMA content.

This result proves that the introduction of DFMA could efficiently reduce the surface energy of the acrylic coating, which was helpful to improve the corrosion resistance of the coating. Fu[25] not only introduce a fluoromonomer into the polymerization of acrylic acid, but also add a polyurethane to the polymerization emulsion, and the resulting modified hydrophobic angle is as high as 113.14°. This value is higher than the results of this study because of the difference in polymer monomer properties, but the improvement of hydrophobic properties of fluoromonomers is unquestionable.

3.4 Thermal stability

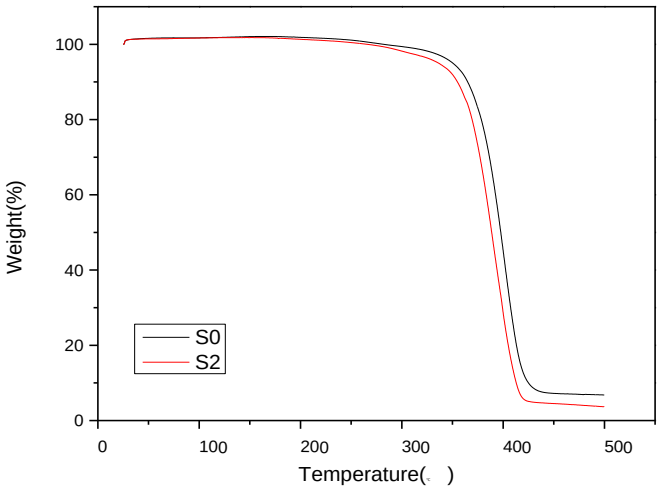

Figure 6. TGA curves of polyacrylate coating (S0) and fluorine-modified coating (S2) coating.

TGA analysis method was utilized to analyze the heat resistance of the modified coating. Fluorine-containing S2 sample and non-fluorine S0 sample were used for comparative analysis. The obtained results were presented in the Figure 6. The initial pyrolysis temperature and the termination temperature of sample S2 was 282°C,472°C. Respectively the initial pyrolysis temperature of sample S0 was 266°C, and the termination temperature was 482°C. The heat resistance of the modified coating increased by 16°C. The reason is that fluorine-containing chains not only have good heat resistance, but also protect other chains.

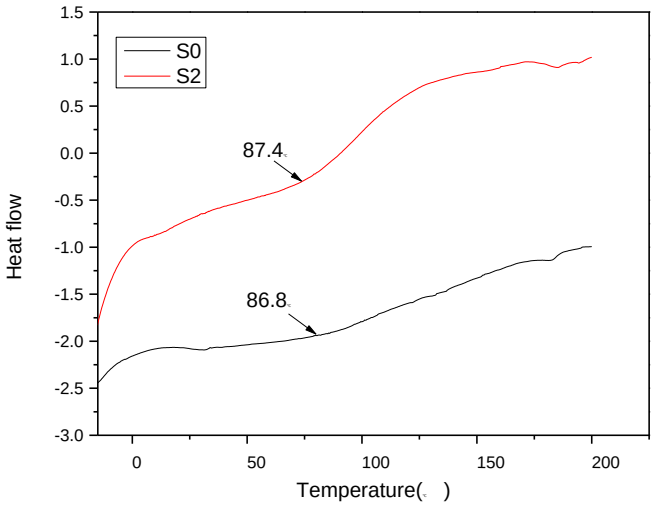

Figure 7. DSC curves of polyacrylate coating (S0) and fluorine-modified coating (S2) coating.

The cross-linking degree was another important parameter for judging the barrier property of the coating, and the degree of cross-linking of the coating could be determined by the glass transition

temperature(Tg) shown by the DSC curve[26,27]. The higher the degree of coating cross-linking was the better the barrier to corrosive ions. Figure 7 showed the DSC curve of the acrylate latex film before and after the fluorine modification. The results showed that the Tg of the sample S2 was higher than that of the S0 sample, introduction of DFMA the degree of cross-linking of the fluorine modified coating was extended. The densification of fluorinated acrylic coating was more dense that the barrier property was better. This also committed the results observed by EDS. The increase of Tg value was related to the intermolecular free volume and intermolecular interactions. The introduction of DFMA enhanced the intermolecular interactions and the intermolecular free volume decreased resulted in an increase in the Tg value. Li et al[28] studied the effect of the amount of AA on the heat resistance of the emulsion. As the amount of AA increased, the Tg of the emulsion also increased. This indicates that not only the fluorine monomer will affect the crosslinking performance of the emulsion, but AA is also acceptable. From the effect, the content of AA may have a greater influence on the crosslinking performance. The effect of AA on the thermal stability of the emulsion is negligible.

3.5 Corrosion resistance analysis

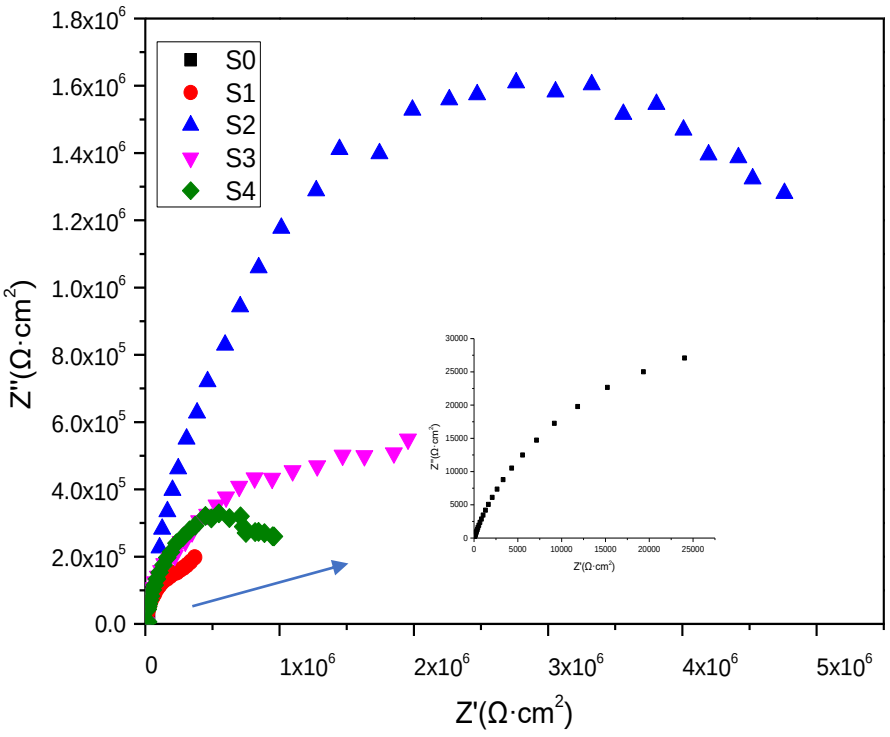

Figure 8. Nyquist plots of different DFMA content coatings after immersion in 3.5wt%NaCl solution for 4h.

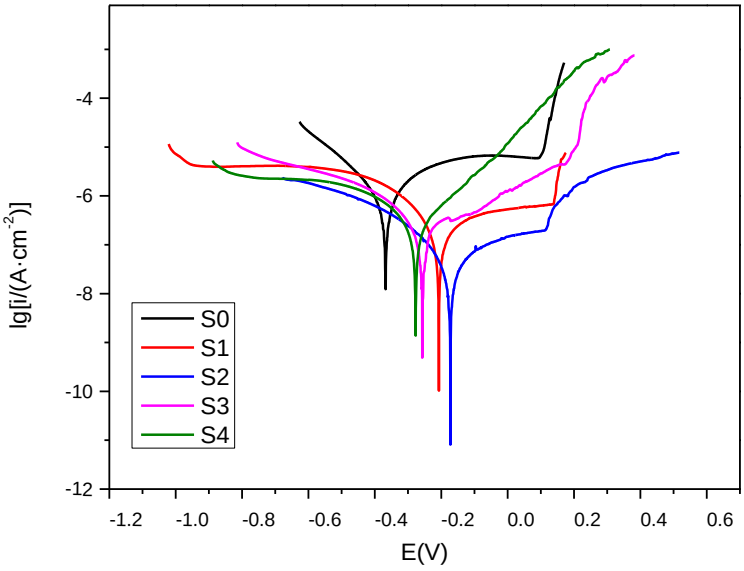

Figure 9. Polarization curves of different DFMA content coatings after immersion in 3.5wt%NaCl solution for 4h.

Table 3. Data of corrosion potential, corrosion current with corrosion rate for different DFMA content coatings by polarization curve fitting.

Sample	I_0(Amp/cm^2)	E_0(V)	Corrosion Rate(mmPY)
S0	2.50E-6	-0.46	0.0027
S1	3.60E-7	-0.21	0.0042
S2	5.54E-8	-0.17	0.00065
S3	6.88E-7	-0.26	0.0081
S4	6.86E-7	-0.28	0.0081

In order to determine the effect of DFMA content on the corrosion resistance of the coatings, the EIS measurements of samples S0 to S1 were performed after soaking in a 3.5 wt% NaCl solution for 4 h. The resulting Nyquist diagram was shown in Figure 8. Compared to the impedance spectrum of the S0 sample without DFMA added, the impedance arc of the DFMA sample was significantly improved. This showed that the addition of DFMA effectively enhanced the corrosion resistance of the coating. From the impedance spectroscopy analysis, the impedance arc increased and decreased with increasing DFMA content. For sample S2, the higher resistance value indicated that it had the best corrosion effect. Figure 9 showed the polarization curve under the same conditions. It could be observed in the figure that compared with the polarization curve of the S0 sample without DFMA added, the DFMA-added sample was entirely shifted to the lower right with a higher corrosion potential and a lower corrosion current density. The corrosion current (Icorr) and corrosion potential (Ecorr) were determined by numerical fitting of the resulting polarization curves with the Butler-Volmer equation. Icorr and Ecorr were extracted by computer programs using a Levenberg/Marquardt nonlinear least-squares fitting method.

The extracted data was shown in Table 3. The S2 sample had a minimum current density of 5.54×10^{-3} A/cm^2. The S0 sample had a maximum current density of 2.50×10^{-6} A/cm^2. In comparison, the corrosion current density of the DFMA sample added was more than three orders of magnitude higher than that of the non-added DFMA sample. The corrosion current densities of S1, S3 and S4 samples were lower than that of S2 samples, which was consistent with the results obtained by impedance spectroscopy. The same EIS test proved that the fluorine-containing emulsion has better corrosion resistance than the fluorine-free emulsion[29]. However, the phosphate ester in the raw material can passivate the metal substrate, but the experimental results show that the corrosion resistance is similar to this paper.

S2 samples were taken for immersion at different times, and the resulting EIS plots were shown in the Figure 10c. Analysing the impedance spectroscopy could show that within 32 hours, with the increase of the immersion time, the impedance arc showed a different degree of increase. We analyzed whether the addition of DFMA resulted in the appearance of this result, so the same immersion experiment was performed on other samples as shown in the figure 10b(d). S1 and S4 samples also showed the same conditions, but the impedance arcs of the S0 and S4 samples did not change much. It could be concluded that the amount of DFMA added affects the corrosion resistance of the coating at different immersion times from this. The impedance arc of the S1 sample reached a maximum value at the immersion time of 16 h, after which the impedance arc began to decrease. The impedance values of the S2 and S3 samples reached maximum at 32 h, and the impedance arc at each time was higher than that of the S1 sample. It could also be seen that the amount of DFMA added in a certain range was positively correlated with the corrosion resistance. The impedance arc of the S4 sample with the largest DFMA content was maintained at the same arc before soaking for 32 h, and a significant drop occurred when the immersion time reached 48 h. It could be seen from the SEM image that the surface of the sample without DFMA had obvious defects and its impedance arc was close to the bare steel impedance arc. So it could be speculated that it basically had no protective effect on the substrate. Due to the presence of a large amount of carboxyl groups in the polyacrylic coating, the hydrophilicity of the coating was strong, and therefore the voids at the defects could even accelerate the intrusion of water and accelerated the corrosion[30].

The impedance spectrum of a typical sample S2 after DFMA addition was fitted. The impedance diagram for different immersion times could be described by the circuit diagrams in the Figure 10f. Rs, Rc, and Rt in the figure represented solution resistance, coating resistance, and charge transfer resistance. Rs indicated the blocking effect of the corrosive environment on the charge transfer. Since the solution was the same and its resistance value differs greatly from the coating resistance, it could be neglected. The Rc and Rt values were approximately the same when immersed for 4 h and 8 h. However Rc of the immersion time reached 16h was equivalent to the aforementioned, but the resistance of Rt increased by nearly two orders of magnitude. Although the surface of the coating after the addition of DFMA becomes denser, there are still some defects. In the initial stage of the immersion, the corrosive ions were corroded through contact with the substrate at the defect.

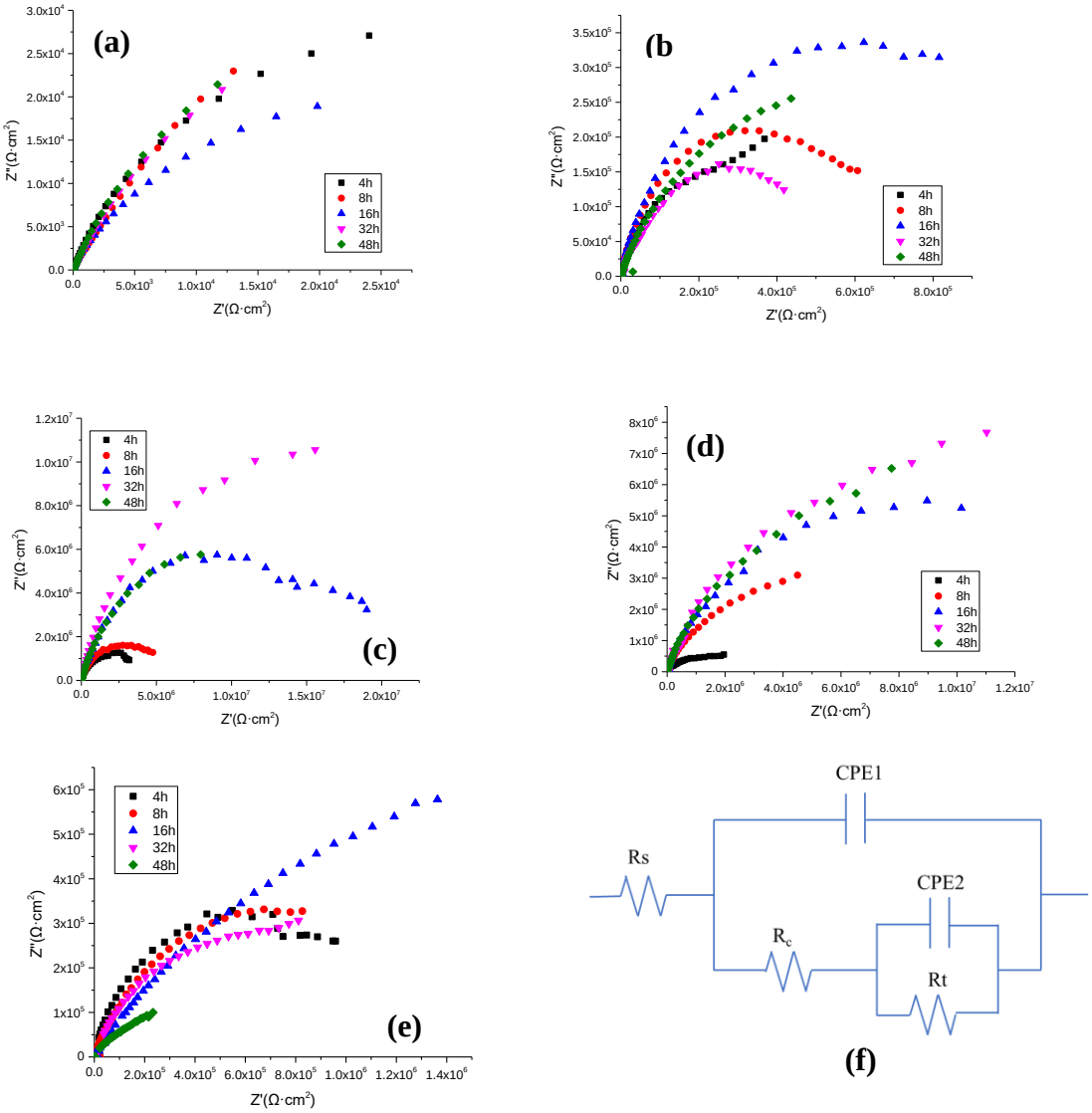

Figure 10. Nyquist plots of S0 coating (a), S1 coating (b), S2 coating (c), S3 coating (d), S4 coating (e) after different immersion time and fitting circuit diagram (f).

Due to the enrichment of fluorine, the surface of the coating modified by DFMA had a large amount of fluorine. It was better hydrophobicity than the unmodified coating surface. Compared with the unmodified coating S0, the anti-corrosion performance of the modified coating had been significantly improved. As the corrosion reaction proceeds, the corrosion product film was formed on the surface of the substrate, and the corrosion reaction was inhibited. When the immersion time reached 16 hours or more, the value of Rt had been significantly improved. Impedance testing was performed on bare steel and fitted, its resistance value was comparable to that of Rt. Which also proved that the increase of Rt value was related to the substrate corrosion product film. When the immersion time exceeded 32 hours, the overall impedance of the coating begins to show a decreasing trend. According to the circuit data of S2 sample impedance arc fitting, the decrease of the impedance arc of the whole coating was due to the decrease of Rc value. The Rc value dropped by nearly two orders of magnitude. This was due to the coating starting to fail, a large number of water molecules invade the substrate. Which could also be seen

from the increase in Rt value when immersion 48h that the substrate began to appear a larger area of corrosion. So Rt value was nearly two orders of magnitude higher than before. It could be concluded that the increase in the immersion anticorrosion performance of the DFMA-modified coating increased first and then decreased, due to the combined effect of the coating defected and the corrosion product film of the substrate. This phenomenon only occurs when the DFMA content is less than 4.12%, and the coating sample not modified by DFMA cannot protect the matrix due to its high hydrophilicity.

Table 3. Data of Rs, Rc and Rt for different DFMA content coatings by Nyquist plots fitting.

Immersion time (h)	Rs ($\Omega \cdot cm^2$)	R_c ($\Omega \cdot cm^2$)	Rt ($\Omega \cdot cm^2$)
4	385.9	4.94E6	101.6
8	447.6	3.61E6	305.5
16	474.1	1.56E6	2.10E4
32	466.3	3.73E7	5.84E4
48	468.6	2.13E5	8.81E6

The addition of DFMA excess S4 sample, although from the perspective of the surface hydrophobicity was slightly higher than the amount of the sample with a lower addition. But its protective performance of the metal substrate was indeed lower than other added samples. The cause of this phenomenon might be due to the difference in adhesion of the coating to the substrate. As we all know, fluoropolymers have a very low surface tension, and the fluorinated segments migrated to the surface of the coating during film formation to reduce the surface tension of the coating. After the addition of excess fluoropolymer, the fluorine-containing segment of the coating interface with the substrate increases. This affects the contact between acrylic polymer segments and the substrate, thus reducing the adhesion of the coating[31].

3.6 Morphologies of the corroded surface beneath the coating

The surface corrosion morphology before and after the coating immersed was shown in the figure11. Before immersion (Fig. 11a), the surface of the coating was smooth and dense, and the surface morphology was not changed after immersion for 8 h (Fig. 11b). The white spherical objects in the figure were unwashed NaCl particles. A cross-linked tubular protrusion appeared on the surface of the coating after immersing for 48 hours (Fig. 11c), indicating that the water had penetrated into the surface of the substrate in large quantities, and the adhesion of the coating began to decrease.

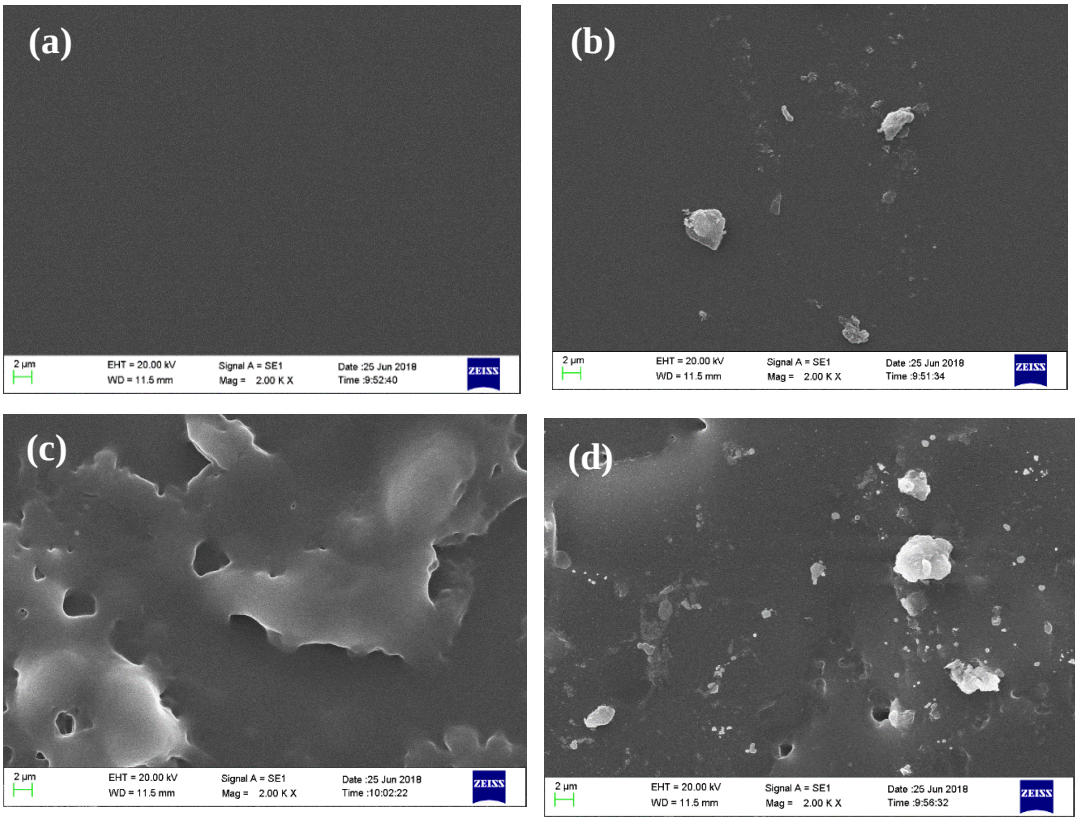

Figure 11. SEM images of samples immersed in 3.5wt% solution for different time, 0h (a), 8h (b), 48h (c), 64h (d).

This also confirms the overall drop in the impedance of the coating after 48 h of immersion in the impedance spectrum. A large number of corrosion pits appeared on the surface of the coating after immersion for 64 hours. Water and corrosive ions could easily immerse into the substrate and corrode.

4. CONCLUSION

The core-shell structure fluorine-modified acrylate emulsion was successfully prepared by seed emulsion polymerization. The preparation properties of the coating on 304 stainless steel were analyzed. The addition of DFMA could improve the crosslinkability, heat resistance and hydrophobicity of the acrylic coating. The corrosion resistance of the modified coating was also greatly increased. Compared to non-fluorinated coating, Ecorr increased from -0.46V to -0.17V, and Icorr decreased by more than two orders of magnitude. The long-term immersion test of the modified coating showed that the corrosion resistance of the coating was an upward trend of early immersion, which was a characteristic phenomenon of the modified coating. In this experiment, the S2 sample had the best corrosion resistance while its DFMA addition amount was only 2.36%. Successfully obtained better coating anti-corrosion performance with lower fluorine content. In short, the fluorine-modified acrylate emulsion with core-shell structure not only has a great improvement in performance, but also has a low cost. It has great potential for development in terms of anti-corrosion.

ACKNOWLEGEMENTS
This work was supported by the National Natural Science Foundation of China（No.51774242.）

References

1. S.G. Wang, M. Sun and K. Long, *Engineering*, 9 (2017) 1.
2. J.H. Sim, Y.S. Kim and I.J. Cho, *Nucl. Eng. Technol.*, 49 (2017) 769.
3. H. Hassannejad and A. Nouri, *J. Mol. Liq*., 254 (2018) 377.
4. P. Rodic, I. Milosev, M. Lekka, F. Andreatta and L. Fedrizzi, *Prog. Org. Coat*., 124 (2018) 286.
5. A.U. Ammar, M. Shahid, M.K. Ahmed, M. Khan, A. Khalid and Z.A. Khan, *Materials*, 11 (2018) 332.
6. P.Y. Bian, X.D. Shao and D.J. Li, *China Surface Engineering*, 31 (2018) 88.
7. G.S. Dhole, G. Gunasekaran, T. Ghorpade and M. Vinjamur, *Prog. Org. Coat*., 110 (2017) 140.
8. S. Qiu, C. Chen, M. Cui, W. Li, H. Zhao and L. Wang, *Appl. Surf. Sci*., 407 (2017) 213.
9. N. Wang, Y. Zhang, J. Chen, J. Zhang and Q. Fang, *Prog. Org. Coat*., 109 (2017) 126.
10. H. Jin and W. Xu, *Coatings*, 8 (2018) 31.
11. J. Wu, J.H. Liou, C.Y. Shu, Y. Patel, R. Menon, C. Santucci, S.T. Iacono, D.W. Smith and B.M. Novak, *React. Funct. Polym*., 93 (2015) 38.
12. Y. Hongyan, Z. Yunhe, Y. Kaiyuan, L. Yu, S. Ying, L. Shanyou and G. Shaowei, *React. Funct. Polym*., 82 (2014) 58.
13. S.F. Zhang, Y.F. He, R.M. Wang, Z.M. Wu and P.F. Song, *Iran. Polym. J*., 22 (2013) 447.
14. B. Weng, D. Shang, L.J. Jin, X.Y. Sun and J.Z. Hang, *Acta. Polym. Sin*., 6 (2017) 990.
15. S.P. Rodrigues, M. Evaristo, S. Carvalho and A. Cavaleiro, *Appl. Surf. Sci*., 445 (2018) 575.
16. J. Zhou, X. Chen, H. Duan and J. Ma, *Polym. Int*., 64 (2015) 1373.
17. T. Lv, D.M. Qi, D. Zhang, Q. Liu and H.T. Zhao, *React. Funct. Polym*., 104 (2016) 9.
18. K. Li, X. Zeng, H. Li and X. Lai, *J. Appl. Polym. Sci*., 132 (2015) 37.
19. W. Xu, Q. An, L. Hao, D. Zhang and M. Zhang, *Appl. Surf. Sci*., 373 (2013) 268.
20. W. Yang, L. Zhu and Y. Chen, *Colloid. Polym. Sci.*, 1 (2015) 293.
21. J.I. Amalvy, M.J. Percy, S.P. Armes and H. Wiese, *Langmuir*, 1007 (2001) 17.
22. B. Wang, Z.M. Wu, D.W. Zhang, R.M. Wang, P.F. Song, Y.B. Xiong and Y.F. He, *Prog. Org. Coat.*, 118 (2018) 122.
23. F. Yu, Y.Y. Hu and C.C. Zhang, *Technology*, 10 (2014) 15.
24. J.W. Ha, I.J. And and S.B. Lee, *Macromolecules*, 38 (2005) 736.
25. J.P Fu, X.J. Lai, X.R. Li, D.N. Zhang and R.H. Mu, *Journal Functional Materials*, 47 (2016) 1234.
26. S. Radhakrishnan, N. Sonawane and C.R. Siju, *Prog. Org. Coat*., 64 (2009) 383.
27. G. Ruhi, O.P. Modi and S.K. Dhawan, *Synthetic Metals*, 200 (2015) 24.
28. K.Q. Li, X.R. Zeng, H.Q. Li and X.J. Lai, *J. Appl. Polym. Sci*., 132 (2015) 37.
29. Y.F. Li, J.J. Zhu, X.H. Gao and Z.M. Yu, *J. Polym. Sci. Pol. Chem*., 50 (2013) 248.
30. H.S. Lin, M. Luo, Y.H. Chen, J. Chen, Z. Wang and P.F. Fang, *Materials Protection*, 48 (2015) 47.
31. Y. Chen, Z.K. Pan and J. Chen, *Surface Technology*, 46 (2017) 26.